

## Exotic Compact Objects and the Fate of the Light-Ring Instability

Pedro V. P. Cunha<sup>1</sup>, Carlos Herdeiro<sup>1</sup>, Eugen Radu<sup>1</sup> and Nicolas Sanchis-Gual<sup>2,1</sup>

<sup>1</sup>*Departamento de Matemática da Universidade de Aveiro and Centre for Research and Development in Mathematics and Applications (CIDMA), Campus de Santiago, 3810-183 Aveiro, Portugal*

<sup>2</sup>*Departamento de Astronomía y Astrofísica, Universitat de València, Dr. Moliner 50, 46100 Burjassot (València), Spain*



(Received 12 August 2022; accepted 6 December 2022; published 7 February 2023)

Ultracompact objects with light rings (LRs) but without an event horizon could mimic black holes (BHs) in their strong gravity phenomenology. But are such objects dynamically viable? Stationary and axisymmetric ultracompact objects that can form from smooth, quasi-Minkowski initial data must have at least one *stable* LR, which has been argued to trigger a spacetime *instability*; but its development and fate have been unknown. Using fully nonlinear numerical evolutions of ultracompact bosonic stars free of any other known instabilities and introducing a novel adiabatic effective potential technique, we confirm the LRs triggered instability, identifying two possible fates: migration to nonultracompact configurations or collapse to BHs. In concrete examples we show that typical migration (collapse) timescales are not larger than  $\sim 10^3$  light-crossing times, unless the stable LR potential well is very shallow. Our results show that the LR instability is effective in destroying horizonless ultracompact objects that could be plausible BH imitators.

DOI: 10.1103/PhysRevLett.130.061401

*Introduction.*—A few years after the first gravitational wave detection from a collision of two black holes (BHs) [1] and the first image of a BH resolving its horizon scale structure [2], there is a scientific consensus about the physical reality of BHs. Yet, both the inability to observationally prove the “*BH hypothesis*” [3–6] and its challenging and far-reaching theoretical consequences [7–9], demand a thorough scrutiny of its alternatives.

In this spirit, a variety of horizonless exotic compact objects (ECOs) have been proposed [10]: the “*ECO hypothesis*.” Any putative ECO model must overcome theoretical and observational tests to become a contender. Of special interest are *ultracompact* ECOs (UCOs, for short), i.e., possessing light rings (LRs): planar bound photon orbits that asymptotically flat BHs must possess [11]. UCOs can imitate the (initial) ringdown [12,13] and (to some extent) the shadow [14] of BHs making them plausible BH foils *if* they are dynamically viable.

Conditions for dynamical viability include (i) a plausible formation mechanism, (ii) sufficient stability against the ubiquitous astrophysical perturbations, and (iii) embedding in a physically sound effective field theory. It was shown in [15] that, under generic assumptions, an equilibrium UCO that forms from smooth, quasi-Minkowski initial data, must have at least a pair of LRs, one of which is stable. It has been argued that the existence of stable LRs can trigger a spacetime instability, by trapping massless perturbations that eventually pile up and backreact on the spacetime [16–18]. The development and fate of this hypothetical generic obstruction to UCOs has, however, been so far unknown.

In this Letter we present the development and fate of the LR instability in concrete models, providing evidence that UCOs with a plausible formation mechanism are destroyed in astrophysical timescales, therefore questioning their viability as BH alternatives.

*UCOs and stable LRs.*—Consider equilibrium, finite Arnowitt-Deser-Misner (ADM) mass  $M$ , asymptotically flat, UCOs described by a stationary, axially symmetric, circular metric [19],  $g_{\mu\nu}$ . In  $(t, r, \theta, \varphi)$  coordinates, such that  $\partial_t$  and  $\partial_\varphi$  are the commuting Killing vectors adapted to stationarity and axisymmetry, respectively, (see Refs. [11,15] for details), the effective *dimensionless* potentials

$$V_{\pm} = \frac{g_{t\varphi} \mp \sqrt{g_{t\varphi}^2 - g_{tt}g_{\varphi\varphi}}}{g_{\varphi\varphi}} M, \quad (1)$$

determine LRs (if they exist) as critical points:  $\nabla V_{\pm} = 0$ . The  $\pm$  sign is connected to the LRs rotation sense.

One can associate a topological charge,  $\mathcal{Q}_i$  to individual LRs [11,15]. The total spacetime topological charge  $\mathcal{Q} = \sum_{\text{LRs}} \mathcal{Q}_i$  is then invariant under smooth spacetime deformations preserving the asymptotic structure and internal regularity. This means that any horizonless, asymptotically flat, everywhere regular UCO has the same topological LR charge as Minkowski spacetime,  $\mathcal{Q} = 0$ . Since unstable (stable) LRs have  $\mathcal{Q}_i = -1$  ( $\mathcal{Q}_i = +1$ ), this implies that in the dynamical formation of UCOs LRs emerge as a stable-unstable pair. This conclusion does not depend on the specific (metric) theory of gravity or on the details of the (incomplete) gravitational collapse [20]. It implies that for

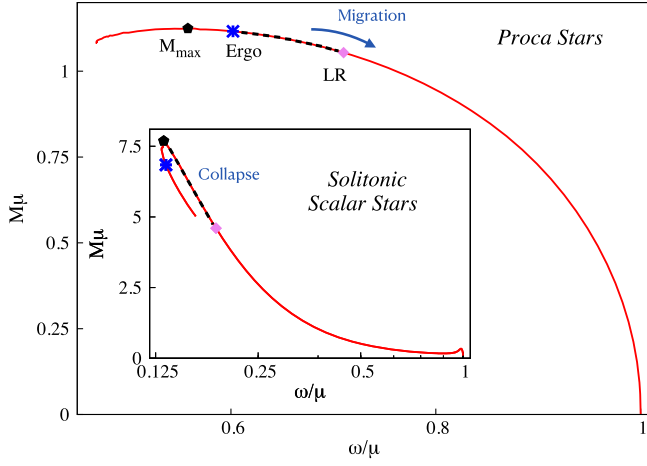


FIG. 1. Space of solutions for model 1 (main panel) and model 2 (inset). Starting at  $\omega/\mu = 1$  and moving leftwards along the solutions curves, one encounters the first solution with a LR (ergoregion) at the pink diamond (blue star). The maximal mass BS, at which an unstable mode is expected to appear (see, e.g., [38]) is marked with a black pentagon.

UCOs with a plausible formation mechanism, the existence of a (Schwarzschild-like) unstable LR—as to imitate BH phenomenology—is accompanied by a potentially dangerous stable LR.

*Adiabatic effective potential.*—We wish to follow the dynamics of UCOs. It has been argued that the instability triggered by stable LRs is nonlinear [16]. Unveiling its final state, moreover, requires a nonlinear analysis. Thus, we shall resort to numerical evolutions of appropriate UCO models, using a 3 + 1 spacetime split:

$$ds^2 = -N^2 dt^2 + \gamma_{ij}(dx^i + \beta^i dt)(dx^j + \beta^j dt), \quad (2)$$

where  $N$  is the lapse function,  $\beta$  is the shift, and  $\gamma$  is the projected three-metric on the  $t = \text{constant}$  slice  $\Sigma_t$ , which uses Cartesian-like coordinates  $\{x, y, z\}$ .

To monitor the evolution of LRs we introduce, from the numerical evolution 3 + 1 data in (2), an adiabatic effective potential (AEP) analog to (1) at *each* time step, taking  $M$  in (1) to be  $M_t$ , the UCO mass at each time slice  $t$ , to allow comparisons at different  $t$ . The AEP carries physical information if the evolution is sufficiently slow and departures for axial symmetry are mild. The lack of stationarity and axisymmetry can, moreover, be washed away by appropriate averaging procedures.

A detailed discussion of the assumptions in constructing the AEP is given in the Supplemental Material [21] (SM)—Sec. I; here we state the key ones: (i) At each  $t$ , approximate Killing vectors  $\partial_t$  and  $\partial_\phi$  exist for the evolving, asymptotically flat and approximately circular UCO. This implies that at each point a  $\lambda \in \mathbb{R}$  exists such that  $\partial_\phi = \lambda\beta$ . (ii)  $\partial_\phi$  is assumed to be tangent to surfaces with  $x^2 + y^2 \equiv r^2 = \text{constant}$  (but  $r$  needs not be a geometric distance). At each  $t$

the coordinate center  $\mathcal{O}: (x, y) = (0, 0)$  is linearly shifted to the UCO center, to account for a possible (slow) drift of the star, which indeed occurs in the examples below. (iii) The evolving UCO is assumed to possess a  $\mathbb{Z}_2$  reflection symmetry around the equatorial plane surface  $z = 0$ .

Under these assumptions, the  $(g_{tt}, g_{t\phi}, g_{\phi\phi})$  data necessary for the AEP (1) is obtained from the 3 + 1 data in (2),  $(N, \beta, \gamma)$  as follows (see SM, Sec. I, for details). (1)  $g_{tt} = -N^2 + \gamma_{ij}\beta^i\beta^j$ ; (2)  $g_{\phi\phi}$  determines the perimeter  $\mathcal{P}$  of a circumference  $r = \text{constant}$ ,  $\mathcal{P} = 2\pi\sqrt{g_{\phi\phi}(r)} = \int_0^{2\pi} \sqrt{\gamma_{xx}y^2 - 2\gamma_{xy}xy + \gamma_{yy}x^2} d\phi$ , where the auxiliary coordinate  $\phi$  is defined via  $x = r \cos \phi$ ,  $y = r \sin \phi$ , and may differ from  $\phi$ . Computing  $\mathcal{P}$  numerically via this integral, yields  $g_{\phi\phi}$ ; (3) since  $g_{t\phi} = g_{\phi\phi}\beta^\phi$ , then  $g_{t\phi} = \pm \sqrt{g_{\phi\phi}}\sqrt{\gamma_{ij}\beta^i\beta^j}$ . The sign is positive (negative) if  $\beta^y > 0$  ( $\beta^y < 0$ ) when  $y = 0$ .

Finally, two averaging procedures are used: (1) To wash away (mild) axial-symmetry deviations, we work with averaged functions over surfaces with  $r = \text{constant}$ , e.g.,  $\langle N^2 \rangle \equiv (1/2\pi) \int_0^{2\pi} N^2 d\phi$ . Then,  $\langle g_{t\phi} \rangle \equiv \pm \sqrt{g_{\phi\phi}} \sqrt{\langle \beta \cdot \beta \rangle}$ , and  $\langle g_{tt} \rangle \equiv -\langle N^2 \rangle + \langle \beta \cdot \beta \rangle$ . (2) To wash away oscillations in the UCO's time evolution around a trend, we introduce time-averaged potentials  $V_\pm^*$ :  $V_\pm^*(r, t) = [2T(t)]^{-1} \int_{t-2T(t)}^t V_\pm(r, \tau) d\tau$ , where  $T(t)$  is a measure of the oscillation period of the lapse  $N(t)$ , taken to represent physical oscillations of the evolving UCO.

*Testing UCO dynamics with bosonic stars (BSs).*—Testing the dynamical viability of UCOs, requires models obeying conditions (i) and (iii) in the *Introduction*, to then assess the impact of LRs on condition (ii). The former are obeyed in families of bosonic stars (BSs) [22,23], which can form via gravitational cooling [24,25] and emerge in simple and robust effective field theories involving scalar or vector fields minimally coupled to Einstein's gravity [26], where numerical evolutions are under control [30]. Additionally, our analysis requires UCO models free of other instabilities (e.g., perturbative or from ergoregions), which would mask the impact of LRs. This rules out the simplest, spherical scalar/vector BSs, which only become UCOs in a perturbatively unstable regime [31].

We have identified two appropriate models of BSs for studying the LR instability, both described by the Lagrangian density,  $\mathcal{L} = R/(16\pi G) + \mathcal{L}_m$ , where  $R$ ,  $G$  are the Ricci scalar and Newton's constant [32]. Model 1 has  $\mathcal{L}_m = -\mathcal{F}_{\alpha\beta}\bar{\mathcal{F}}^{\alpha\beta}/4 - \mu^2 A_\alpha \bar{A}^\alpha/2$ , describes a complex Proca model with mass  $\mu$  [33], and we focus on its fundamental, spinning, mini-Proca star solutions [34,35]. They are labeled by their ADM mass  $M$  or their oscillation frequency  $\omega$  and are dynamically robust [36]. These Proca stars become UCOs for  $\omega/\mu \lesssim 0.711$ ; an ergoregion emerges for  $\omega/\mu \lesssim 0.602$  and perturbative instabilities are expected beyond the maximal  $M$ , for  $\omega/\mu \lesssim 0.562$ —Fig. 1

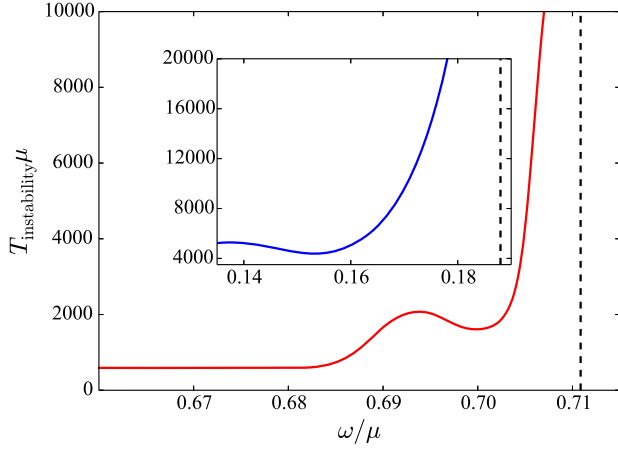


FIG. 2. Instability timescale for model 1 (main panel) and model 2 (inset). The dashed vertical line marks the first UCO.

(main panel). Model 2 has  $\mathcal{L}_m = -\partial_\alpha \Phi \partial^\alpha \bar{\Phi} - \mu^2 |\Phi|^2 [1 - 2|\Phi|^2/\sigma_0^2]^2$ , describes a self-interacting complex scalar model with mass  $\mu$  and coupling  $\sigma_0$ . We focus on its fundamental, spinning, solitonic boson star solutions [37,38], again labeled by  $M$  or  $\omega$ , choosing the illustrative value  $\sigma_0 = 0.05$  [39]. There is a dynamically robust relativistic branch of solutions for  $\omega/\mu \lesssim 0.493$  [38], that become UCOs for  $\omega/\mu \lesssim 0.188$ ; perturbative instabilities are expected beyond the maximal  $M$ , for  $\omega/\mu \lesssim 0.132$  and the ergoregion appears in this unstable branch for  $\omega/\mu \lesssim 0.134$ —Fig. 1 (inset) [40].

The just described Proca (solitonic boson) stars in the range  $0.602 < \omega/\mu < 0.711$  ( $0.132 < \omega/\mu < 0.188$ ) provide tests for the LR instability (dashed line segments in Fig. 1). Using them as initial data, we have performed fully nonlinear numerical evolutions of the Einstein-bosonic systems with spacetime variables in the Baumgarte-Shapiro-Shibata-Nakamura formulation and the EINSTEIN TOOLKIT [42,43] evolved using MCLACHLAN [44,45] and LEAN [46]—codes available in [47] and described in [31,48,49].

*Results model 1: migration.*—We have evolved the aforementioned Proca stars up to  $t\mu = 10^4$  and confirmed the existence of an instability for the UCOs. Figure 2 (main panel) shows the time at which the instability starts vs  $\omega$  [50]. The timescale tends to diverge when approaching the first star with a LR ( $\omega/\mu \simeq 0.711$ ), thus associating the instability with UCOs. For some of the models with LRs we could not see the development of instability, since the simulations last only up to  $t\mu = 10^4$  but our results suggest that they will become unstable if evolved for longer. The instability is not seen for stars with  $\omega/\mu > 0.711$ .

To grasp the nature of the instability, Fig. 3 shows snapshots of the time evolution of the energy density on the equatorial plane for stars with  $\omega/\mu = 0.68, 0.69, 0.70$ , and angular momentum density for  $\omega/\mu = 0.68$ . The energy density first acquires an octagonal shape (see second row of Fig. 3) which evolves into a “starfishlike” pattern (third

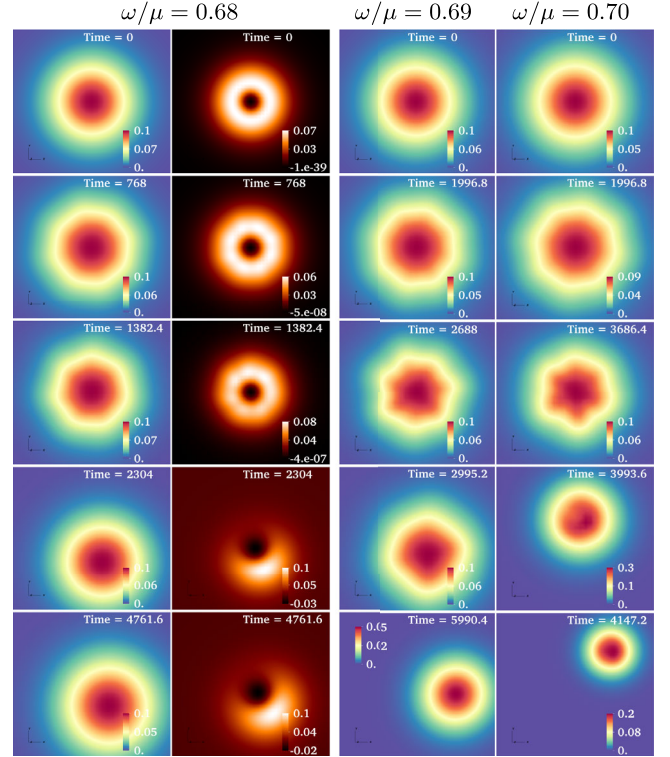


FIG. 3. Snapshots of the energy density (and angular momentum density in middle left column) of three spinning Proca star UCOs with  $\omega/\mu = 0.68$  (left and middle left column),  $0.69$  (middle right column), and  $0.70$  (right column). Time runs from top to bottom, given in code units.

row). The axisymmetry of the star is mildly broken and the star suffers a small kick, slowly moving away from the grid center. The instability triggers a balanced mass and angular momentum loss, mostly carried by the Proca field, with almost no gravitational wave emission. This balanced loss allows a migration to less massive and compact but still spinning Proca stars without LRs—see arrow in Fig. 1 and SM (Sec. II) for details.

Further clear evidence that the fate of this instability is a non-UCO spinning Proca star is obtained by examining the averaged AEP  $V_-^*$  [51]. At each time slice, this potential has the typical radial profile for an UCO displaying a stable and an unstable LR [Fig. 4 (top, inset)] from which one can extract a potential depth  $h$ , defined as the (positive) potential difference of  $V_-^*$  computed at the LRs.  $h$  can be represented as a function of time in the evolutions. Figure 4 (top) shows it for  $\omega/\mu = 0.68$ . It is clear that the depth  $h(t)$  reaches zero at  $t_c\mu \simeq 7480$ , i.e., the two LRs have merged in a finite time. This merger is further seen on the bottom panel of Fig. 4, where the perimetral radius of both LRs converges to a single value. After this point the LRs essentially disappear in terms of  $V_-^*$ . However, for a limited couple of instances right after  $t > t_c$  the LRs can be recreated and destroyed again due to sporadic fluctuations of the potential (not shown in Fig. 4), before disappearing

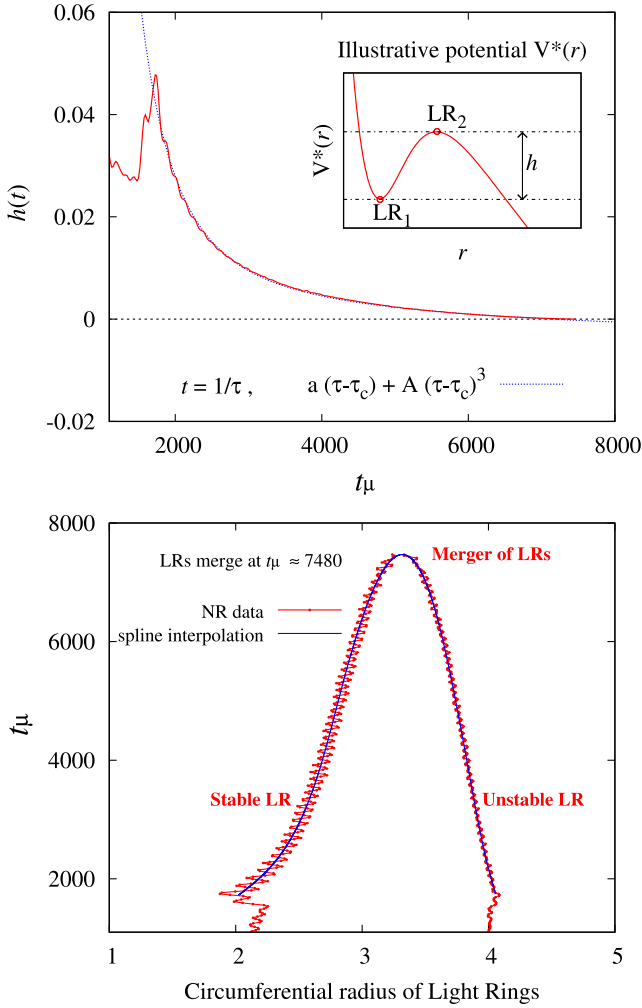


FIG. 4. Top: potential-well depth  $h$  (illustrated in inset) as a function of time for  $\omega/\mu = 0.68$ . A guiding fit function (dotted line) is defined in terms of the inverse time  $\tau = 1/t$ , with adjusted constants  $\{a, A, \tau_c\}$ . Bottom: the LRs' circumferential radii  $\sqrt{g_{\varphi\varphi}}/M_t$  for different values of time  $t$ . The blue line is an auxiliary spline interpolation to help convey the underlying pattern. The time-averaged potential  $V_*$  can suppress several, but not all, oscillation modes of the raw potential  $V_-$ . This is the likely cause of the observed zigzagging of the red curve, a manifestation of residual star radial oscillations around their unexcited state (at that time).

altogether. This confirms the migration robustly evolves in the direction of destroying the LR pair. In the SM (Sec. I), the time evolution of the AEP is further detailed, legitimating the validity of the adiabatic approximation underlying the AEP.

*Results model 2: collapse.*—We have also evolved the spinning solitonic scalar boson stars described above. In the UCO region,  $\omega/\mu \lesssim 0.188$ , we have again observed an instability, absent for  $\omega > 0.188$  (but within the relativistic stable branch). Its timescale again tends to diverge, as we approach the critical frequency [Fig. 2 (inset)], correlating

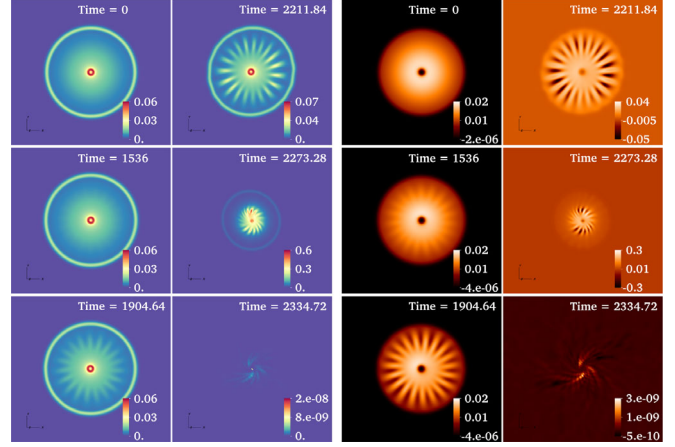


FIG. 5. Time evolution of a spinning solitonic BSs with  $\omega/\mu = 0.16$  which has LRs. (Left and middle left column) Energy density. Time runs from top to bottom and then from left to right. (Middle right and right column) Angular momentum density. Both quantities are extracted on the equatorial plane.

the instability with the existence of LRs. The initial development of the instability qualitatively resembles the previous case in the loss of axisymmetry—see Fig. 5 for evolution snapshots of the star with  $\omega/\mu = 0.16$ . However, the outcome is different; the star collapses and forms a spinning BH, diagnosed by the emergence of an apparent horizon (detailed in the SM—Sec. II). The culprit of this different outcome may be the self-interaction potential, that confines the star and suppresses the dissipation through gravitational cooling, the essential channel by which migration occurs in model 1. The AEP shows violent oscillations and appears to deepen near the location of the stable LR before the collapse, implying the technique loses validity.

*Remarks.*—Proving the BH hypothesis is as challenging as disproving the ECO hypothesis. A smaller, but informative step, is to rule out classes of inadequate models as BH alternatives. The evidence shown in this Letter supports the inadequacy, as BH foils, of a large class of UCOs, for which a plausible formation mechanism exists via an incomplete gravitational collapse of quasi-Minkowski initial data. Even if such UCOs could form as a transient state, their unavoidable stable LR triggers an instability that, generically, develops in a moderate timescale, either promoting collapse to BHs or migration to a non-UCO. It remains to be seen whether UCOs near the critical configuration, for which the timescale can grow (likely) arbitrarily large, still retain any effectiveness as BH foils, and if other fates are possible for the LR instability, e.g., considering different UCO models. It also remains an open problem to find a practical estimate of the LR instability timescale in a generic spacetime. One of our main results is a concrete timescale within two specific models. The difficulty arises from the putative nonlinear character of the instability.

Perhaps some lesson can be taken from other gravitational nonlinear instabilities, namely, the anti-de Sitter (AdS) turbulent instability [52]. In fact, the trapping of modes in the stable LR potential well has some conceptual similarities with the trapping of perturbations in the AdS “box.”

There are mechanisms to avoid the conclusion in [15] that UCOs have stable LRs; e.g., (i) topological non-triviality; e.g., ultracompact wormholes, since such UCOs are not diffeomorphic to Minkowski spacetime. But any mechanism forming such macroscopic UCOs is beyond general relativity and remains to be established; (ii) nonaxisymmetry; but the known astrophysical compact objects exhibit to a high degree axisymmetry; (iii) non-circularity; but very few (analytic or numerical) solutions describing compact objects in Einstein’s or modified gravity without circularity are known.

The ability of ECOs to imitate BH phenomenology does not demand LRs. Examples are known, both for gravitational wave (e.g., [53,54]) and electromagnetic (e.g., [55]) observations, where ECOs without LRs could mimic, in limited circumstances, some strong gravity BH features. It seems implausible, however, that ECOs without LRs may mimic *all* BH phenomenology and replace them entirely as physical players in the Universe. Under this rationale, our results challenge the ECO hypothesis as a complete replacement of the BH hypothesis, but not as another ingredient of the physical Universe.

This work was supported by the Spanish Agencia Estatal de Investigación (Grant No. PGC2018-095984-B-I00 and No. PID2021-125485NB-C21), by the Generalitat Valenciana (PROMETEO/2019/071), by the Center for Research and Development in Mathematics and Applications (CIDMA) through the Portuguese Foundation for Science and Technology (FCT—Fundação para a Ciência e a Tecnologia), references UIDB/04106/2020 and UIDP/04106/2020, by national funds (OE), through FCT, I. P., in the scope of the framework contract foreseen in the numbers 4, 5, and 6 of the article 23, of the Decree-Law 57/2016, of August 29, changed by Law 57/2017, of July 19 and by the projects PTDC/FIS-OUT/28407/2017, CERN/FIS-PAR/0027/2019, PTDC/FIS-AST/3041/2020 and CERN/FIS-PAR/0024/2021. This work has further been supported by the European Union’s Horizon 2020 research and innovation (RISE) programme H2020-MSCA-RISE-2017 Grant No. FunFiCO-777740 and by FCT through Project No. UIDB/00099/2020. P. C. is supported by the Individual CEEC program 2020 funded by the FCT. N. S. G. acknowledges financial support by the Spanish Ministerio de Universidades, through a María Zambrano grant (ZA21-031) with reference UP2021-044, within the European Union-Next Generation EU. Computations have been performed at the Servei d’Informàtica de la Universitat de València, and the Argus and Blafis cluster at the U. Aveiro.

- [1] B. P. Abbott, R. Abbott, T. D. Abbott, M. R. Abernathy, F. Acernese, K. Ackley, C. Adams, T. Adams, P. Addesso, R. X. Adhikari *et al.*, *Phys. Rev. Lett.* **116**, 061102 (2016).
- [2] K. Akiyama *et al.* (Event Horizon Telescope Collaboration), *Astrophys. J.* **875**, L1 (2019).
- [3] E. Berti *et al.*, *Classical Quantum Gravity* **32**, 243001 (2015), arXiv:1501.07274.
- [4] L. Barack *et al.*, *Classical Quantum Gravity* **36**, 143001 (2019).
- [5] K. G. Arun *et al.* (LISA Collaboration), *Living Rev. Relativity* **25**, 4 (2022).
- [6] C. A. R. Herdeiro, arXiv:2204.05640.
- [7] R. Penrose, *Phys. Rev. Lett.* **14**, 57 (1965).
- [8] S. W. Hawking, *Phys. Rev. D* **14**, 2460 (1976).
- [9] A. Almheiri, D. Marolf, J. Polchinski, and J. Sully, *J. High Energy Phys.* **02** (2013) 062.
- [10] V. Cardoso and P. Pani, *Living Rev. Relativity* **22**, 4 (2019).
- [11] P. V. P. Cunha and C. A. R. Herdeiro, *Phys. Rev. Lett.* **124**, 181101 (2020).
- [12] V. Cardoso, E. Franzin, and P. Pani, *Phys. Rev. Lett.* **116**, 171101 (2016); **117**, 089902(E) (2016).
- [13] V. Cardoso and P. Pani, *Nat. Astron.* **1**, 586 (2017).
- [14] P. V. P. Cunha and C. A. R. Herdeiro, *Gen. Relativ. Gravit.* **50**, 42 (2018).
- [15] P. V. P. Cunha, E. Berti, and C. A. R. Herdeiro, *Phys. Rev. Lett.* **119**, 251102 (2017).
- [16] J. Keir, *Classical Quantum Gravity* **33**, 135009 (2016).
- [17] V. Cardoso, L. C. B. Crispino, C. F. B. Macedo, H. Okawa, and P. Pani, *Phys. Rev. D* **90**, 044069 (2014).
- [18] G. Benomio, *Anal. Part. Diff. Eq.* **14**, 2427 (2021).
- [19] In practice, circularity amounts to writing an ansatz which is invariant under the discrete symmetries  $t \rightarrow -t$  and, simultaneously,  $\varphi \rightarrow -\varphi$ , where  $t, \varphi$  are coordinates adapted to the Killing symmetries.
- [20] In particular, the theorem in [15] does not require stationarity and axi-symmetry *during* this incomplete collapse.
- [21] See Supplemental Material at <http://link.aps.org/supplemental/10.1103/PhysRevLett.130.061401> for more details on the assumptions in constructing the AEP and the loss of energy and angular momentum in the numerical evolutions.
- [22] F. E. Schunck and E. W. Mielke, *Classical Quantum Gravity* **20**, R301 (2003).
- [23] R. Brito, V. Cardoso, C. A. R. Herdeiro, and E. Radu, *Phys. Lett. B* **752**, 291 (2016).
- [24] E. Seidel and W.-M. Suen, *Phys. Rev. Lett.* **72**, 2516 (1994).
- [25] F. Di Giovanni, N. Sanchis-Gual, C. A. R. Herdeiro, and J. A. Font, *Phys. Rev. D* **98**, 064044 (2018).
- [26] The nonself-interacting vector model used here is free of known pathologies [27–29].
- [27] K. Clough, T. Helfer, H. Witek, and E. Berti, *Phys. Rev. Lett.* **129**, 151102 (2022).
- [28] A. Coates and F. M. Ramazanoğlu, *Phys. Rev. Lett.* **129**, 151103 (2022).
- [29] Z.-G. Mou and H.-Y. Zhang, *Phys. Rev. Lett.* **129**, 151101 (2022).
- [30] S. L. Liebling and C. Palenzuela, *Living Rev. Relativity* **15**, 6 (2012).

- [31] P. V. P. Cunha, J. A. Font, C. Herdeiro, E. Radu, N. Sanchis-Gual, and M. Zilhão, *Phys. Rev. D* **96**, 104040 (2017).
- [32] We use geometrized units,  $G = 1 = c$  here after.
- [33] Overbar denotes complex conjugation.
- [34] C. A. R. Herdeiro and E. Radu, *Phys. Rev. Lett.* **119**, 261101 (2017).
- [35] C. Herdeiro, I. Perapechka, E. Radu, and Y. Shnir, *Phys. Lett. B* **797**, 134845 (2019).
- [36] N. Sanchis-Gual, F. Di Giovanni, M. Zilhão, C. Herdeiro, P. Cerdá-Durán, J. A. Font, and E. Radu, *Phys. Rev. Lett.* **123**, 221101 (2019).
- [37] B. Kleihaus, J. Kunz, and M. List, *Phys. Rev. D* **72**, 064002 (2005).
- [38] N. Siemonsen and W. E. East, *Phys. Rev. D* **103**, 044022 (2021).
- [39] M. Bezares, C. Palenzuela, and C. Bona, *Phys. Rev. D* **95**, 124005 (2017).
- [40] In both models solutions with ergoregions are UCOs, in agreement with [41].
- [41] R. Ghosh and S. Sarkar, *Phys. Rev. D* **104**, 044019 (2021).
- [42] EINSTEINTOOLKIT, “Einstein Toolkit: Open software for relativistic astrophysics,” <http://einsteintoolkit.org/>.
- [43] F. Löffler, *Classical Quantum Gravity* **29**, 115001 (2012).
- [44] J. D. Brown, P. Diener, O. Sarbach, E. Schnetter, and M. Tiglio, *Phys. Rev. D* **79**, 044023 (2009).
- [45] MCLACHLAN, “McLachlan, a public BSSN code.”
- [46] H. Witek and M. Zilhão, “CANUDA,” <https://bitbucket.org/canuda/>.
- [47] H. Witek, M. Zilhao, G. Bozzola, M. Elley, G. Ficarra, T. Ikeda, N. Sanchis-Gual, and H. Silva (2021), 10.5281/zenodo.3565474.
- [48] M. Zilhão, H. Witek, and V. Cardoso, *Classical Quantum Gravity* **32**, 234003 (2015).
- [49] N. Sanchis-Gual, C. Herdeiro, J. A. Font, E. Radu, and F. Di Giovanni, *Phys. Rev. D* **99**, 024017 (2019).
- [50] The timescale of the instability is set by inspection, when notorious nonaxisymmetric features start to develop.
- [51] For these Proca stars the LRs emerge as critical points of  $V_-$ , rather than  $V_+$ .
- [52] P. Bizon and A. Rostworowski, *Phys. Rev. Lett.* **107**, 031102 (2011).
- [53] J. C. Bustillo, N. Sanchis-Gual, A. Torres-Forné, J. A. Font, A. Vajpeyi, R. Smith, C. Herdeiro, E. Radu, and S. H. W. Leong, *Phys. Rev. Lett.* **126**, 081101 (2021).
- [54] J. Calderon Bustillo, N. Sanchis-Gual, S. H. W. Leong, K. Chandra, A. Torres-Forne, J. A. Font, C. Herdeiro, E. Radu, I. C. F. Wong, and T. G. F. Li, [arXiv:2206.02551](https://arxiv.org/abs/2206.02551).
- [55] C. A. R. Herdeiro, A. M. Pombo, E. Radu, P. V. P. Cunha, and N. Sanchis-Gual, *J. Cosmol. Astropart. Phys.* **04** (2021) 051.